PENETRATION INTO DAMAGED GRANITE*

Dr. Susan Babcock
Applied Research Associates, Inc, PO Box 5388, Albuquerque, NM 87185

Dr. Phil Randles
Defense Threat Reduction Agency, 1680 Texas St SE, Kirtland AFB, NM 87117

ABSTRACT

The Defense Threat Reduction Agency (DTRA) conducted a series consisting of a detonation test and a series of diagnostic penetrations in a weathered granite site at White Sands Missile Range, New Mexico, USA. DTRA had previously investigated the penetrability into damage concrete, which provided baseline data for a relatively homogeneous, well-defined target. For the weathered granite site, one detonation and several penetration tests were completed, with the first two penetration tests shot into the *in situ* weathered granite. The detonation test was then executed to produce a damaged region and was instrumented with velocity gages and accelerometers to measure the ground motions. The following penetration tests were into the post-detonation damaged region at a variety of ranges. Pre and post calculations were performed using two computer codes: SAMPLL, which is a penetration code, and DYNA-2D, which is a first principal code used to calculate the ground motions and damage. A consistent trend was found between the distance from the explosive event and the damage factor for the post-detonation penetration tests. These tests have extended the investigation of damage on penetrability from concrete targets to rock targets, and are important to the modeling efforts for second-projectile penetration into damaged targets. This paper will discuss the testbed layout and characteristics, and will present the instrumentation and damage trend results from these tests.

behavior. However, two major differences between concrete targets and rock targets are that 1) rock is pre-fractured and 2) the rock testbed has no large impedance mismatches with surrounding soil (as did the concrete testbed), behaving more like a semi-infinite target. From some preliminary observations in concrete, a pre-damaged target may result in surprisingly high levels of damage when exposed to additional explosive charges. The pre-fracturing characteristic to various degrees of all rock targets may also produce surprising levels of damage from an explosive charge. However, at this point, we can only guess.

The tests discussed in this report were a series of penetration and detonation events executed in a weathered rock test site. The first two tests were diagnostic penetration tests into the existing weathered granite target. The third test was a detonation event that was configured to be comparable to the explosive event from the concrete test series. The final series of tests were penetration tests into the post-detonation damaged test site. This report discusses the testbed condition and layout, the instrumentation results for the detonation event, the damage trend as measured by the post-detonation penetration tests, and the posttest 2-D DYNA calculations.

2.0 TEST SITE GEOLOGY

Based on seismic refraction results, the geology at the site can be categorized in three basic layers. The upper layer is soil ranging from 0 to 5 ft thick with a mean seismic velocity of 2100 ft/s. The middle layer is weathered and fractured granite averaging 17 ft thick with a mean velocity of 5800 ft/s. The lower layer is still somewhat weathered and fractured. Its depth is unknown (beyond 60 ft) and its mean velocity is around 7700 ft/s.

In addition to the seismic refraction surveys, other types of geologic/material properties characterization efforts were conducted at the site. These efforts included coreholes, standard downhole geophysical logs, downhole velocity logs, portable cone penetrometer tests, geologic site reconnaissance, posttest excavation wall sampling, geology, fracture mapping, and laboratory physical and mechanical property tests on core and hand/excavation samples.

The unconfined compressive strength (f'c) for site is plotted in Figure 2-1. The value for f'c varies from about 2000 psi at a 12-ft depth up to 4500 psi at the 35-40-ft depth. Values of about 5500 psi were measured for some of the samples taken at the 25- and 26-ft depths. Cores that could be tested were not obtained for depths less than 12 ft due to the friable nature of the material.

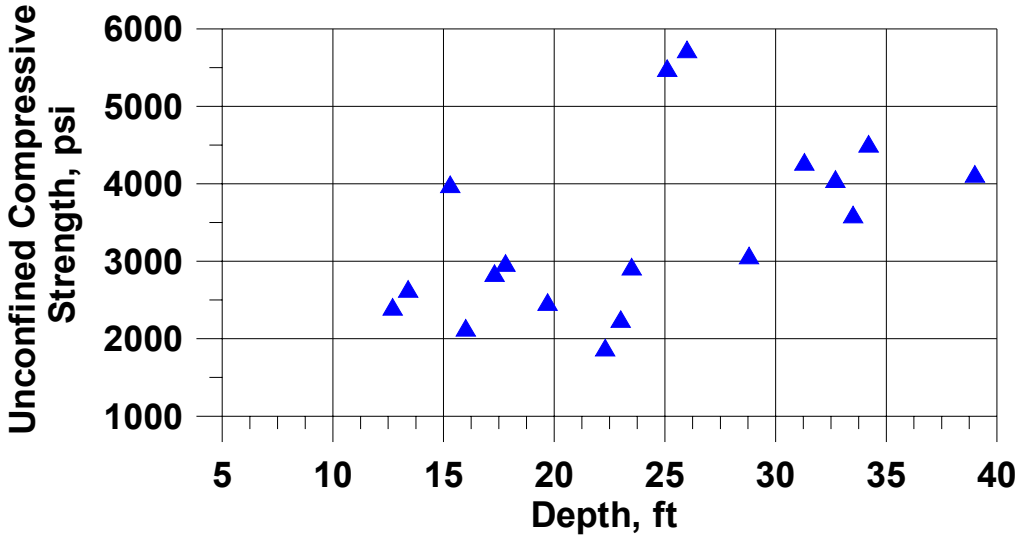

Figure 2-1. Unconfined compressive strength plotted versus depth for intact cores from the weather granite test site.

3.0 TESTBED SETUP

3.1 Overview of Testbed and Testbed Preparations

A diagram of the testbed is shown in Figure 3-1. Ground Zero (GZ) consisted of a 10-ft deep hole lined with a PVC pipe that extended another 10 ft above the testbed surface. A 10-ft berm was placed over the testbed and around the pipe to enhance the coupling of the explosive with the testbed. The explosives were loaded into the pipe up to the 10-ft level. Sandbags were then used to stem the top 10 ft of the pipe.

Six instrumentation holes were cored at 45-deg angles for the placement of the accelerometer and velocity gage canisters. The holes were cored such that the gages would be nominally located at ranges of 4, 8 and 12 ft and a depth of 5 ft (see Figure 3-1).

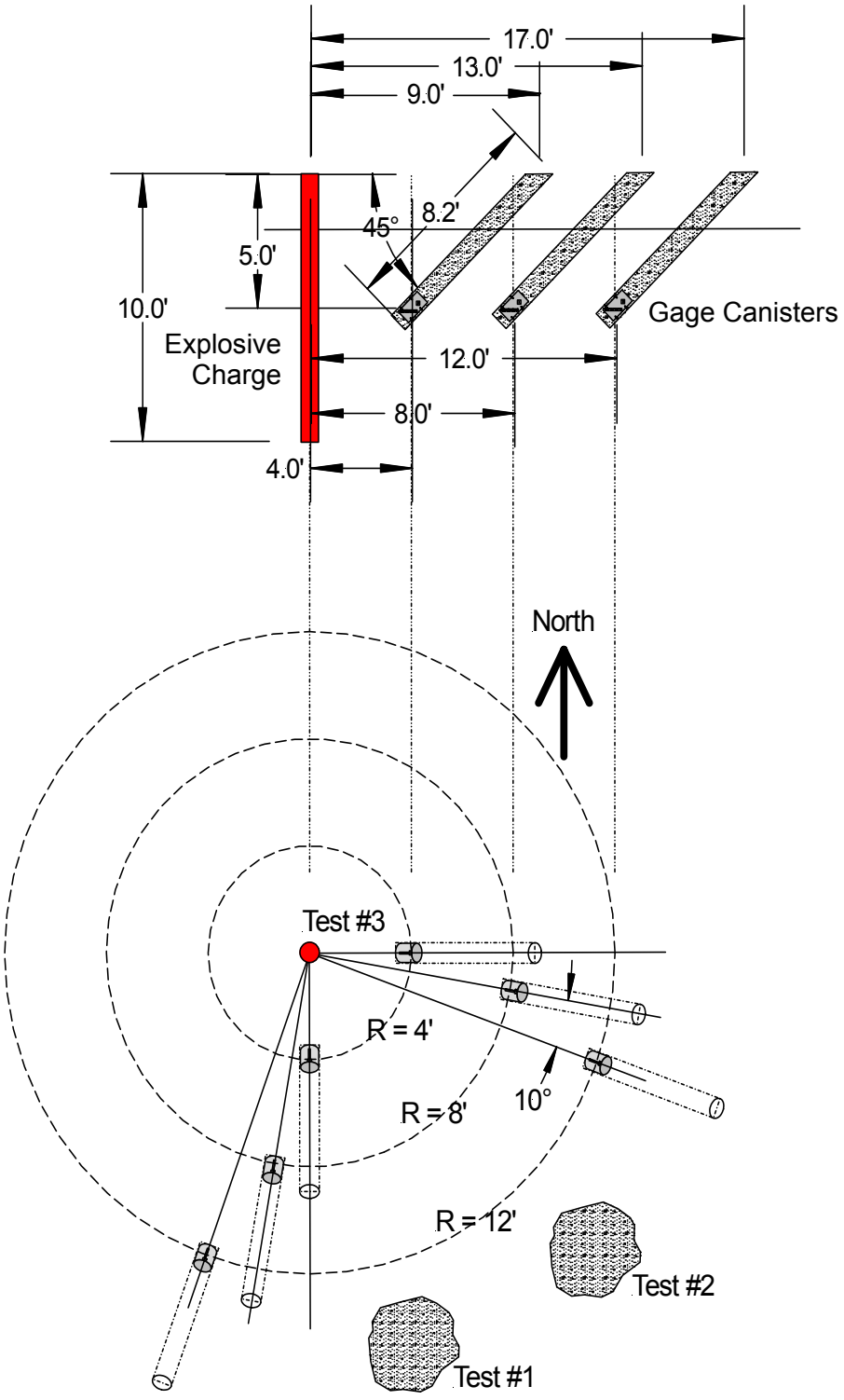

Figure 3-1. Layout of testbed for two penetration events and the detonation event.

3.2 Accelerometers and Velocity Gages

Six velocity gages fabricated by the Sunburst Co. were mounted in canisters together with accelerometers to provide peak velocity and displacement data. Typically, Sunburst gages provide very reliable peak velocity measurement, but their useful recording limit occurs when the magnet inside the gage bottoms out against its canister. The combined use of velocity and acceleration gages allows a baseline correction to the accelerometers based on the velocity records, and obtains longer-time velocity and displacement records than would be allowed by the use of Sunburst gages alone. Figure 3-2 shows a diagram of the canister that includes both a Sunburst gage and an accelerometer.

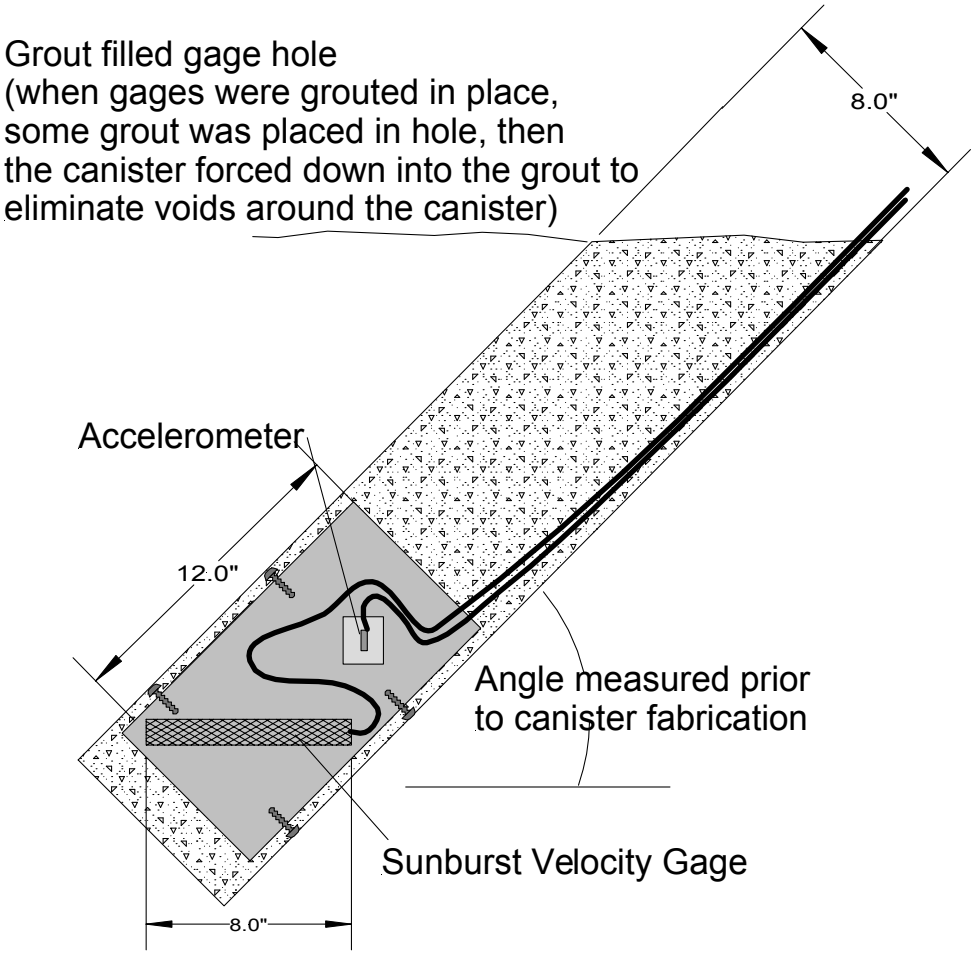

Figure 3-2. Diagram of gage canister position in an instrumentation hole.

4.0 PRETEST PENETRATION PREDICTIONS.

The computer code SAMPLL (References 1 and 2) was used to simulate the penetration of the penetrator into the weathered granite. SAMPLL uses time marching curvilinear algorithms to model the penetrator trajectory through a target. The code assumes the penetrator is a rigid body and divides its surface up into small, discrete areas. The loads on the penetrator surface are determined using empirically based algorithms. These surface loads are summed to determine the penetrator's kinematical response over each time step. The accelerations of the penetrator are integrated over time to determine the penetrator's overall path through the target.

SAMPLL is a two-dimensional penetration code that utilizes a unit-less penetrability S-number to describe the resistance of a target material to a penetrator. The S-number of a target material is proportional to the penetration depth of a penetrator. Materials with a smaller S-number are harder and more difficult to penetrate. A penetrator will penetrate twice as far in a target material with an S-number of 4 than an S-number of 2. Example S-numbers are provided in Table 4-1.

Table 4-1. Example S-numbers for various target materials.

Target Material	Example S-number
Loose top soil	10-20
Sandy gravel, no cementation	4-6
3,000 psi concrete, 1% reinforcement	0.89
5,000 psi concrete, 1% reinforcement	0.76
'Tombstone' granite	0.65

An empirically based equation has been developed by Sandia National Laboratories to determine a rock target's penetrability (Reference 3):

$$S = 12 \ (f'_c * Q)^{-0.3} \qquad \text{(Equation 4-1)}$$

where:

f'_c = Rock unconfined compressive strength, lb/in^2
Q = Unit-less rock quality designator (0.1 – 1.0)

This equation was used to estimate the penetrability of the target material.

The rock at the test site was assumed to be similar to the rock targeted during previous events executed at a different, but similar, weathered granite site. This rock target had two distinct layers. The top layer was made of highly weathered granite and extended 2-4 ft below the ground surface. The lower layer was moderately weathered granite, and was assumed to be infinitely thick. The penetrability of the highly weathered material was defined using Equation 4-1. The rock quality designator (Q) was given a value of 0.3, representing highly to moderately weathered material.

Many of the parameters used in the pretest simulations were randomly varied using a Monte Carlo iterative process. With multiple penetration simulations, the iterative process provided a range of possible test outcomes. The varied parameters were given uniform distributions. Two sets of Monte Carlo penetration simulations were performed. The first set assumed a constant thickness (3 feet) of the upper, highly weathered rock layer. The second set assumed a uniform distribution of the thickness of this upper rock layer. The parameters varied for the SAMPLL Monte Carlo simulations are provided in Table 4-2.

Table 4-2. Parameters varied in the pretest penetration simulations.

Parameter	**Value**
Penetrator impact velocity	1,000 ± 25 ft/s
Penetrator trajectory angle, from the target surface	85° ± 5°
Penetrator angle of attack	0°
Upper Layer: highly weathered rock layer S-number	1.47 ± 0.3
Upper Layer: highly weathered rock layer thickness	First Set: 3.0 ft ± 0.0 ft
	Second Set: 3.0 ± 1.0 ft
Lower Layer: moderately weathered rock layer S-number	0.77 ± 0.15
Lower Layer: moderately weathered rock layer thickness	∞

The results of the pretest penetration simulations are provided in Figure 4-1.

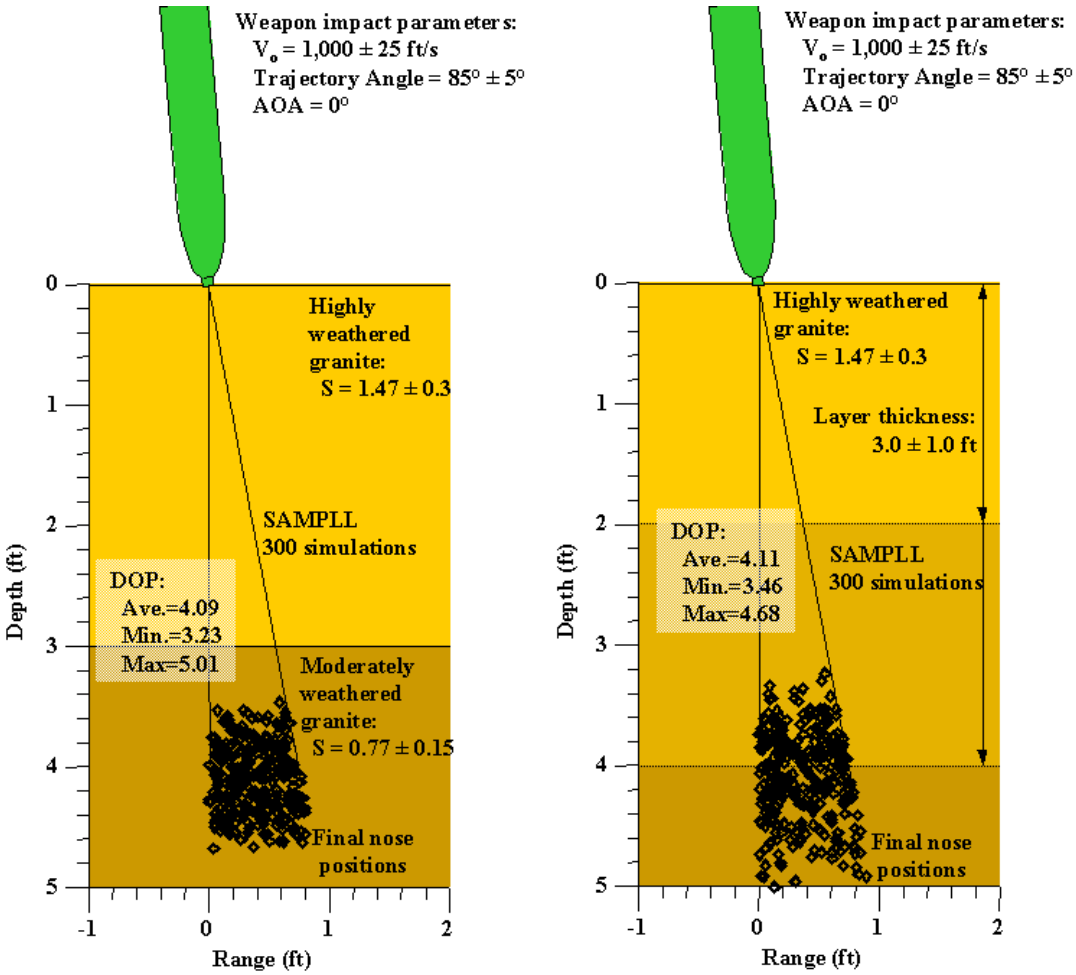

First Set of Calculations Second Set of Calculations

Figure 4-1. Depth plotted versus range for the pretest penetration simulations.

5.0 RESULTS

5.1 Pre-Detonation Penetration Events Results

Two penetration events were completed on June 20, 2001, prior to the detonation event. These two events were conducted in the southern portion of the testbed. The site for these tests was selected such that they would have a minimum impact on the instrumentation, the detonation event, and on the post-detonation penetration events.

The penetration results from these events were very similar, with penetration depths of about 36 in.

5.2 Detonation Event Results

The detonation event was executed on July 19, 2001. This test consisted of an explosive charge that was 10 ft long with 180.96 lbs of QM100RAT (Reference 4).

5.2.1 Testbed surveys

Once the 10-ft berm was removed, the crater region was carefully excavated. Determining the limits of the crater was subjective because of the highly damaged nature of the overall region. A ring of relatively consistent damage around the GZ area was determined by probing with a shovel (Figure 5-1). This ring is shown as the green surveyed points in Figures 5-2, 5-3 and 5-4. Once the ring was marked, the excavation was started using a backhoe. Hand excavation was used to complete the clean-out of the crater region, including a pit near the ground zero (GZ) cavity of the charge. The expected charge cavity appeared to have collapsed and could not be defined during the excavation. However, detonation products were visible in the pit

The region around the crater was carefully cleaned off using compressed air to reveal the fracture patterns and damaged area. A zone around the excavated crater was observed and surveyed and is indicated in orange in the Figures 5-2, 5-3 and 5-4. This zone was highly fractured and had a very rough appearance compared to the smoother, more intact regions of the testbed.

Figure 5-1. Photograph of the excavation of the testbed, showing the use of shovels to help determine the extent of the highly damaged region. The photograph also shows the 3-D surveying systems used through out the tests.

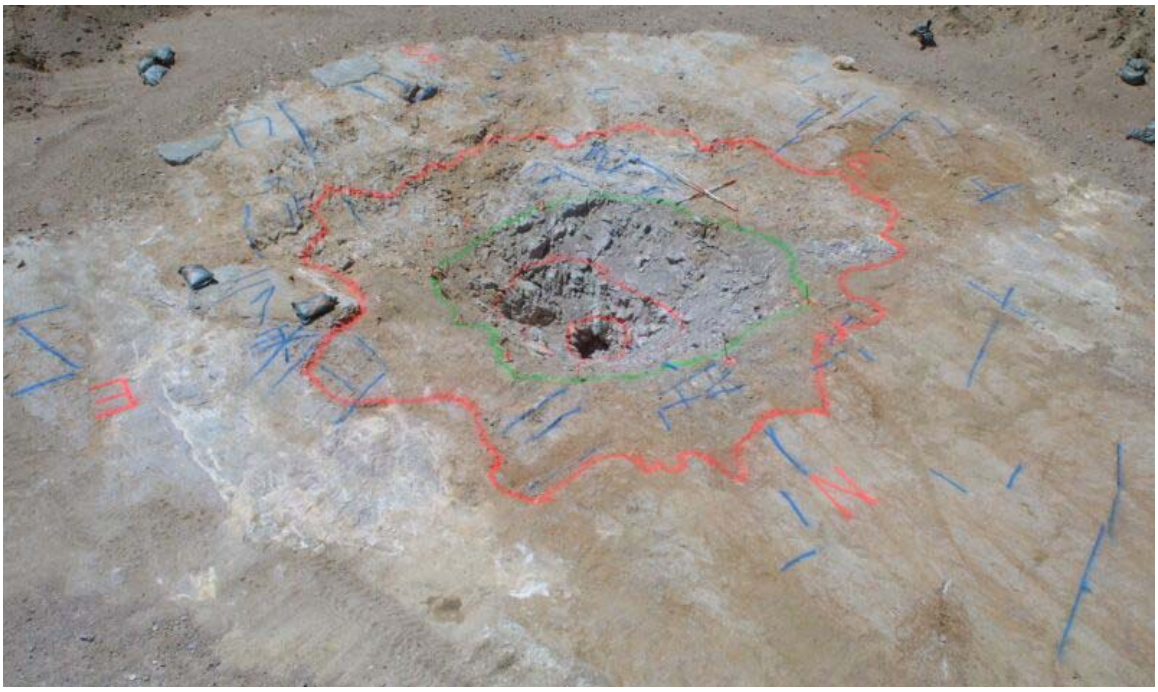

Figure 5-2. Overview photograph of the crater facing SW.

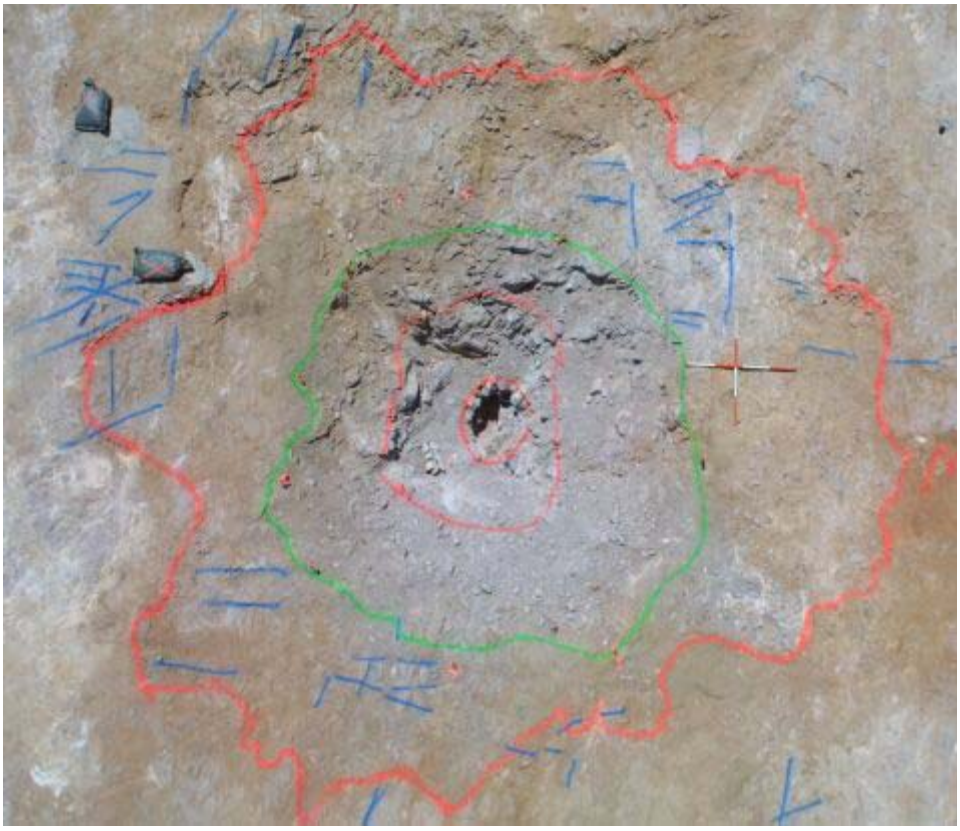

Figure 5-3. Overhead photograph of the crater. North is the bottom of the picture.

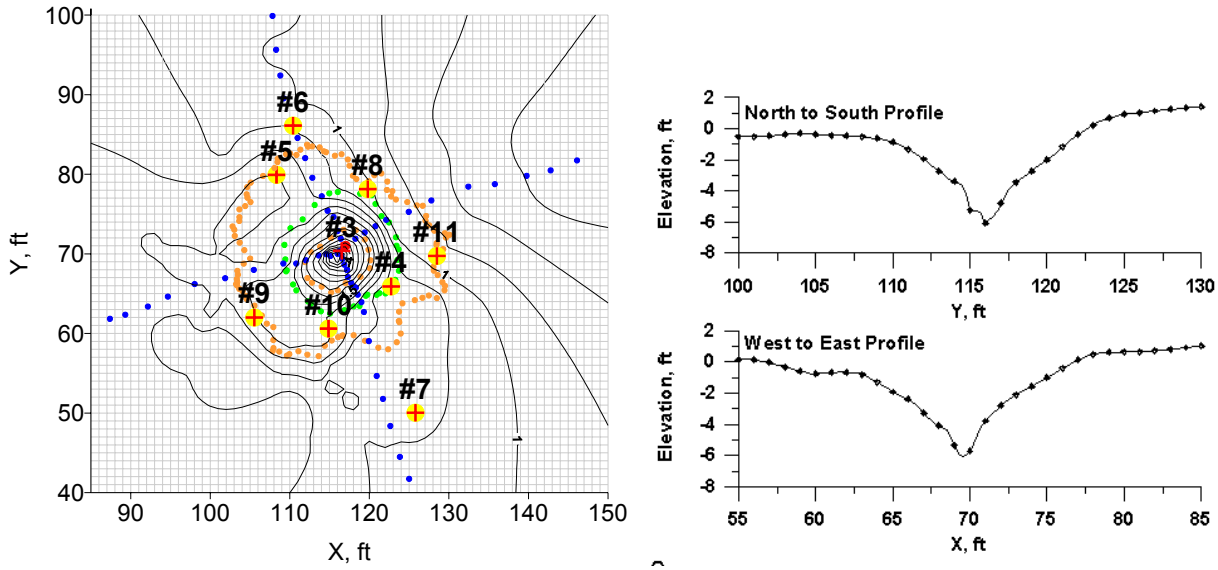

Figure 5-4. Overhead view of contour plot of the crater. The outside orange ring delineates the damaged zone, while the green ring delineates the excavated crater region. The locations for post-detonation penetration tests are also included.

5.2.2 Accelerometer and Velocity Instrumentation Results

Six canisters, Canisters 1 through 6, were placed in the locations shown in Table 5-1. During the placement of the six canisters, the cables for one of the canisters were damaged. This canister containing gages A6 and V6 was located at the 12-ft range and was on the South + 20 deg radial. Other than these two gages, the remaining ten gages recorded data during the detonation event.

Table 5-1. Canister locations relative to GZ.

Canister Number	Range from GZ, ft	Radial
1	4	East
2	8	East + 10 deg
3	12	East + 20 deg
4	4	South
5	8	South + 10 deg
6	12	South + 20 deg

Times-of-arrival of the shock front from all ten gages were obtained and are plotted in Figure 5-5. This plot indicates that a consistent delay in time-zero occurred for all ten channels. The intercept of a linear fit through the acceleration data points, shown on the plot, indicates that the delay was 50.27 msec. Because the accuracy nor the cause of this calculated delay was not known, a rounded value of 50 msec was subtracted from the time for all of the instrumentation records.

The acceleration records are plotted in Figure 5-6. Clipping of the peak is evident on A2, A3, and A4. The relatively minor clipping on A4 was caused by underprediction, but the significant

clipping on A2 and A3 was due to a recording error. The records from A1 and A5 provided usable data with peaks of about 15 kg and 2 kg, respectively.

The velocity records are also plotted in Figure 5-6. Only minor clipping occurred in V1 at about 140 ft/s, while the record from V4 appears to have died shortly after peak velocity was recorded. The records from V2 and V5, which are at the 8-ft range at two different radials, are very similar with peaks of about 30 ft/s. The peak velocity measured by V3 was about 10 ft/s. All of these values were higher than the predicted values, which were 60, 15, and 12 ft/s at 4, 8, and 12 ft, respectively.

A summary of the peak values for the accelerometers and velocity gages is in Table 5-2, with the values plotted in Figure 5-7. A least squares curve fit to velocity data is included on the plot.

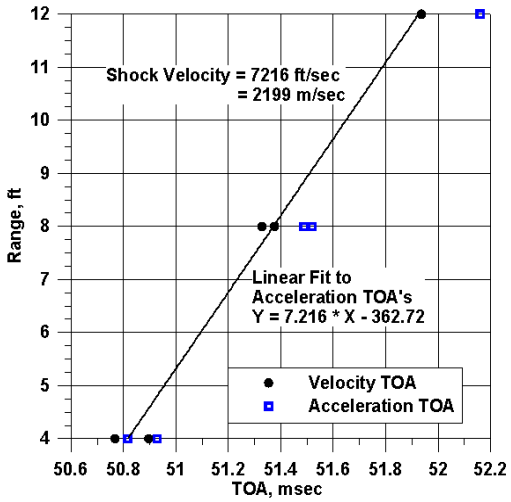

Figure 5-5. Time-of-arrival from the accelerometers and velocity gages. A 50 ms delay for all channels is evident in this plot.

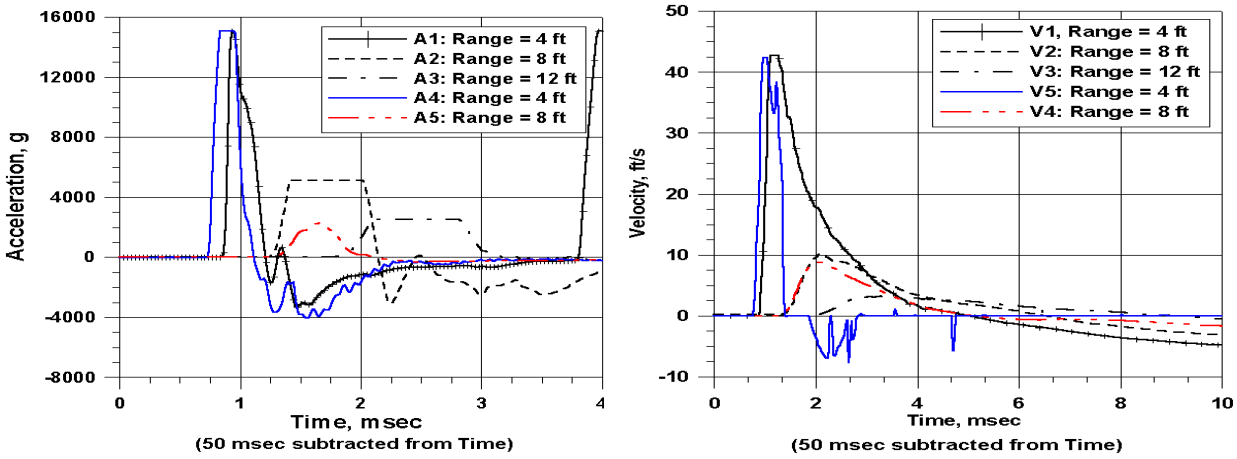

Figure 5-6. Acceleration and velocity histories.

Table 5-2. Summary of instrumentation results for the detonation event.

Gage No.	Radius (ft)	Azimuth (deg)	Distance Below Ground Surface	Peak Accel (g)	Peak Velocity (ft/s)	Time of Arrival (ms)	Comments
Accelerometers							
A1	4	90	5	15067	94.7	0.9	
A2	8	100	5	5094		1.33	clipped
A3	12	110	5	2508		1.94	clipped
A4	4	120	5	15087		0.77	clipped
A5	8	130	5	2273	27.37	1.38	
A6	12	140	5	no data		--	damaged pretest
Velocity Gages							
V1	4	90	5		140.24	0.93	slightly clipped
V2	8	100	5		33.05	1.52	
V3	12	110	5		10.59	2.16	
V4	4	120	5		138.89	0.82	slightly clipped
V5	8	130	5		28.74	1.49	
V6	12	140	5		no data	--	damaged pretest

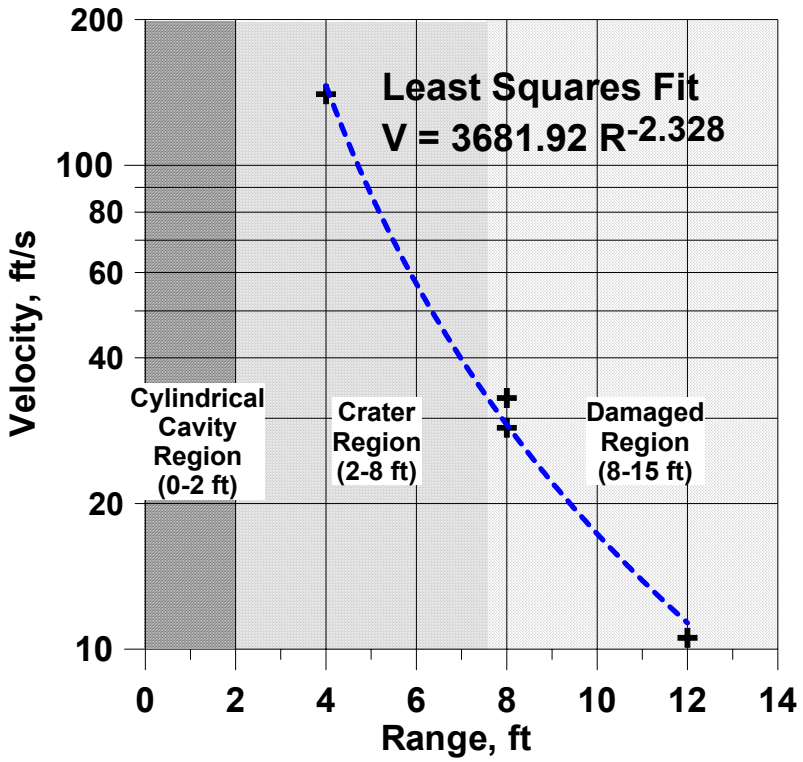

Figure 5-7. Range versus peak velocity. Included on this plot is a power curve for the attenuation of the velocity data.

5.3 Post-Detonation Penetration

The damage trend versus range developed from the penetration data is shown in Figure 5-8. The damage trend was developed using normalized penetration data obtained around the detonation event. A clear correlation between distance from the detonation event and the damage was observed.

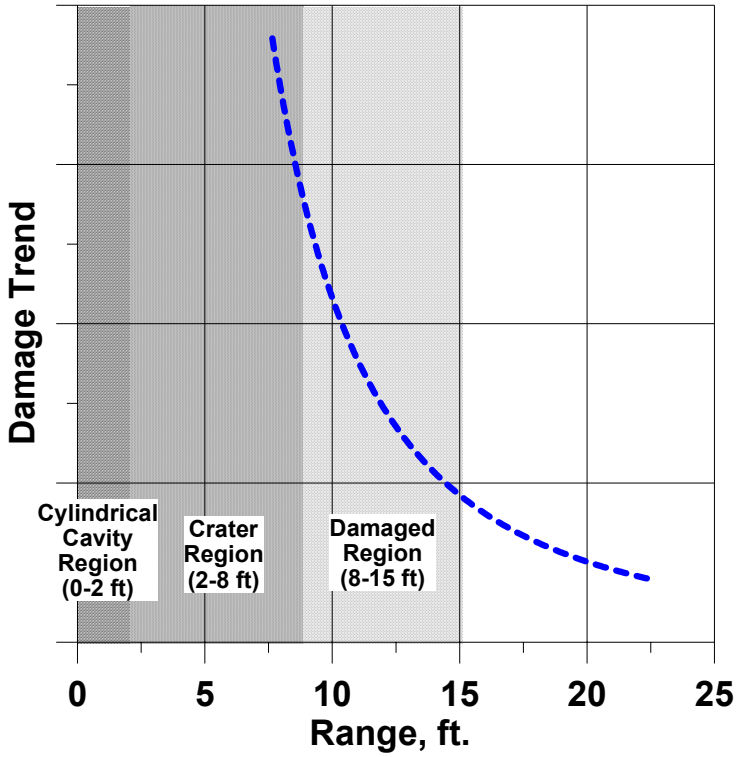

Figure 5-8. Damage trend versus range.

6.0 FINITE ELEMENT MODEL

The finite element code DYNA-2D was used to perform numerical simulations of the detonation event. The explosive source was modeled as a cavity void with an initial explosive volume of 3,073 in^3. The pressure on the explosive cavity wall was determined from time-dependent Jones-Wilkes-Lee (JWL) (Reference 5) equations with the following values for associated coefficients estimated for QM100RAT. Note that these coefficients are based on theoretical calculations and have not been verified by experiment:

Initial Detonation Energy	E_o	=	0.051 tera-ergs/cc
After Burn Energy	Q_o	=	0.057 tera-ergs/cc
After Burn Release Rate	α	=	0.0065 per μ-second
	R_1	=	4.5
	R_2	=	1.0
	A	=	5.1

$$B = 0.044$$
$$\omega = 0.35$$

The Applied Engineering Cap Model with Three Invariants (AEC-3I, Reference 6) was used to model both the pretest and posttest rock models for the finite element calculations. The posttest *in situ* granite model was built to provide the best possible fit to the measured test data from the detonation event.

Figure 6-1 shows the distribution of damage to the host materials for the posttest calculations. The red zone shown in the figure represents the 100% damaged material, which has no residual compressive strength. This is the type of material that was excavated from the crater. The crater profile for the excavated region is included in the figure. Comparing the crater profile with the 100% damage zone indicates that the calculation is predicting slightly too large of a 100% damage zone. The green region of damage in the figure represents about 40 to 60% damaged. The unconfined compressive strength for this material damaged to the 50% level is about one-half of the virgin material, which would be about 1300 psi for the green region. Below 20% damage, the material has only strain "hardened" and has not reached the ultimate compressive strength, so the light blue region would be expected to still have the full unconfined compression strength of about 2600 psi. From the figure, the material would be expected to remain at full strength at ranges from GZ greater than about 12 ft at the surface. From the penetration tests, the material did not reach full compressive strength until more than 22 ft from GZ. Future efforts will be expended to better define the damage conditions in the field at depths down to 20 ft and compare them to the calculated values.

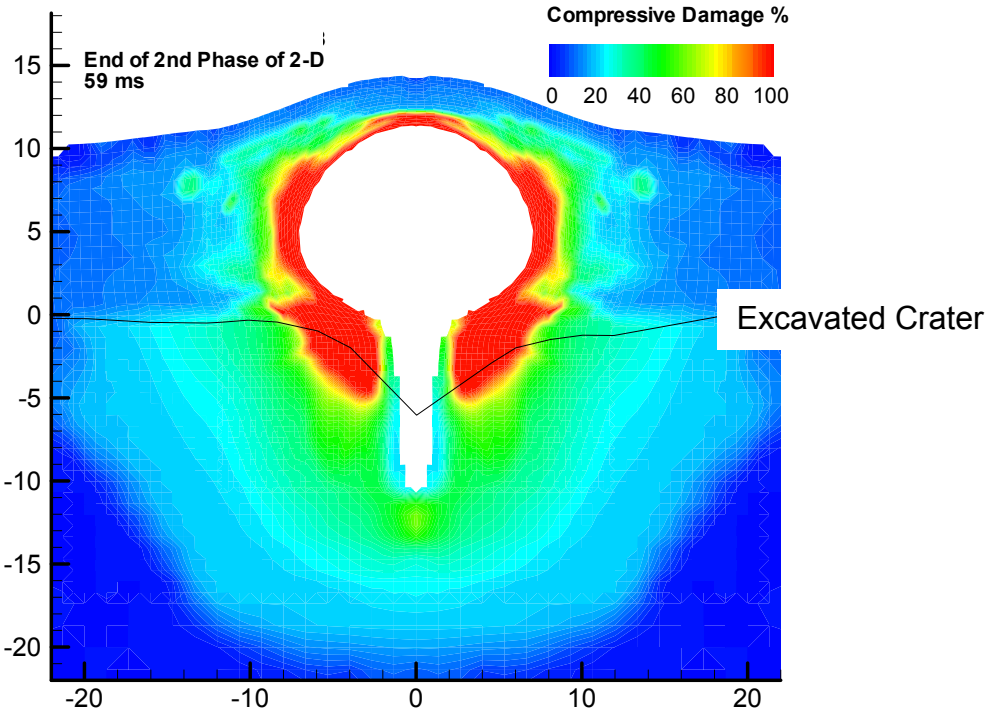

Figure 6-1. Damage distribution from the DYNA-2D posttest calculation.

7.0 SUMMARY AND CONCLUSIONS

This test series was a very successful series of penetration and detonation events executed in a weathered granite target.

Since ground motions such as particle velocity are relatively well-calibrated quantities for many rock types, relating the penetrability and damage to the peak particle velocity is of special interest. These trends were developed from the least square fit equations for damage trend versus range (Figure 5-8). The resulting trend is shown in Figure 7-1. This trend will be evaluated with respect to on-going calculations for a follow-on test. Three-dimensional calculations will use the selected material model from the 2-D calculation discussed in this report and expand for a second detonation 15 ft from the detonation event location.

The penetration data from this effort will be extended with on-going efforts. The first effort is to correlate the penetration to sounding results from a Rotary Percussion Sounding System, which will be used to identify the layering at the site. Correlation to mechanical properties of the rock will also be made if possible. In addition, a follow-on test series is planned to determine the effect of a second, near-by, detonation and subsequent penetration. A final effort is proposed to investigate the effect of damage on penetration for a material with a higher intact strength. This test series will help determine the dependence of damage on the intact material properties.

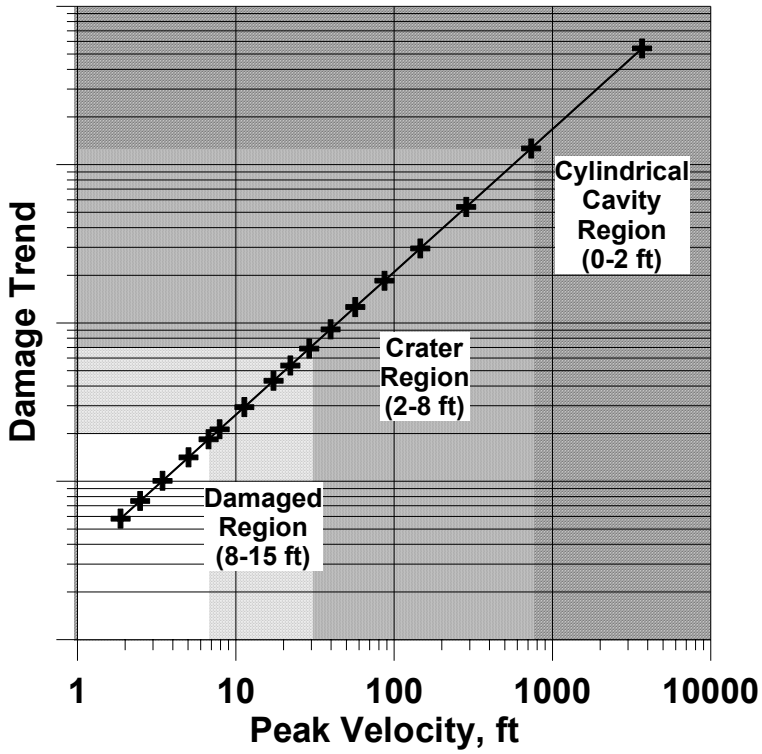

Figure 7.1 Damage versus peak velocity for detonation test.

8.0 REFERENCES

1. Young, C. W., "Simplified Analytical Model of Penetration with Lateral Loading User's Guide," SAND98-0978, Sandia National Laboratories, Albuquerque, NM, May 1998.

2. Young, C. W., "Equations for Predicting Earth Penetration by Projectiles: An Update," SAND88-0013, Sandia National Laboratories, Albuquerque, NM, July 1988.

3. Young, C. W., "Penetration Equations Update – January 1995," internal report, Applied Research Associates, Inc., 4300 San Mateo Blvd. NE, Suite A-220, Albuquerque, NM 87110, January 1995.

4. Babcock, S. M. and J. R. Rocco, "Aluminized Explosives Tests Series 7-12 Results Report," POR 7638, Defense Threat Reduction Agency, Dulles, VA, October 2000.

5. Dobratz, B., "Properties of Chemical Explosives and Explosives Simulants," UCRL-51319, Revision 1, Section 8, Lawrence Livermore National Laboratory, Livermore CA, July 1974.

6. Bingham, B. L., "Applied Engineering Cap Model with Three Invariants," internal report, Applied Research Associates, Inc., 4300 San Mateo Blvd, NE, Suite 220, Albuquerque, NM 87110, 1995.